

Extension of the Brinkman-Rice picture and the Mott transition*

Hyun-Tak Kim**

Telecom. Basic Research Lab., ETRI, Taejeon 305-350, Korea

In order to explain the metal-Mott-insulator transition, the Brinkman-Rice (BR) picture is extended. In the case of less than one as well as one electron per atom, the on-site Coulomb repulsion is given by $U = \kappa\rho^2 U_c$ by averaging the electron charge per atom over all atomic sites, where κ is the correlation strength of U , ρ is the band filling factor, and U_c is the critical on-site Coulomb energy. The effective mass of a quasiparticle is found to be $\frac{m^*}{m} = \frac{1}{1-\kappa^2\rho^4}$ for $0 < \kappa\rho^2 < 1$ and seems to follow the heat capacity data of $\text{Sr}_{1-x}\text{La}_x\text{TiO}_3$ and $\text{YBa}_2\text{Cu}_3\text{O}_{7-\delta}$ at $\kappa = 1$ and $0 < \kappa\rho^2 < 1$. The Mott transition of the first order occurs at $\kappa\rho^2 = 1$ and a band-type metal-insulator transition takes place at $\kappa\rho^2 = 0$. This Mott transition is compared with that in the $d = \infty$ Hubbard model.

PACS number(s): 71.27.+a, 71.30.+h, 74.20.Mn, 74.20.Fg

Although several theoretical studies have been performed to reveal the mechanism of the metal-insulator transition (MIT),¹⁻⁴ the Mott MIT (called "Mott transition") in 3d transition-metal oxides including strongly correlated high- T_c superconductors still remains to be clarified.^{5,6} In particular, the effective mass near the Mott transition has attracted special attention because it is related to both the mechanism of the MIT and the two-dimensional density of states (2D-DOS). The latter offers a clue to explain the mechanism of high- T_c superconductivity.

In this paper, we build an extended BR picture with a generalized effective mass depending on the carrier density, which reduces to the BR picture in the case of one electron per atom, and apply it to experimental data of $\text{Sr}_{1-x}\text{La}_x\text{TiO}_3$ and YBCO.

In strongly correlated metals with one electron per atom on a $d = \infty$ simple cubic lattice, the on-site Coulomb repulsion U is always given. However, in real metallic crystals, in which the number of electrons n is less than the number of atoms m , U is determined not uniquely but instead by probability, because the electronic band structure between sites differs and this system does not transform from real-space to K -space. Therefore, when charges on a site are averaged over all atomic sites, U can be defined, such as in the case of one electron per atom.

In the case when $n = m$, the existence probability ($P = n/m = \rho = \rho_\uparrow + \rho_\downarrow$, "the band filling factor") of electrons on nearest neighbour sites is one. The on-site Coulomb interaction of two electrons in the conduction band is given by $U = U' \equiv \langle \frac{e^2}{r} \rangle$. In the case when $n < m$, $P < 1$ and the on-site charge is $e' = eP$ (or $e'/e = P$), when averaged over sites. Then, the Coulomb energy is given by $U = P^2 U'$. U' does not necessarily agree with the critical value $U_c = 8|\bar{e}|$ of the interaction in the BR picture.¹ The Coulomb repulsion is thus given by

$$U = P^2 U' = \rho^2 U', \quad (1)$$

$$U' = \kappa U_c, \quad (2)$$

$$U = \kappa \rho^2 U_c, \quad (3)$$

where $0 < \rho \leq 1$, while $0 < \kappa \leq 1$ is the correlation strength. In the case of $\kappa \neq 1$ and $\rho = 1$ ($\rho_\uparrow = \rho_\downarrow = \frac{1}{2}$), U reduces to the correlation in the BR picture. In the case when $\kappa = 1$ and $\rho \neq 1$, U tends to U_c when the band approaches half filling. This indicates that having more carriers in the conduction band increases the correlation, *vice versa*.

Although U in the Hubbard model is replaced by Eq. (1), calculations of the expectation value of U based on the Gutzwiller variational theory⁷ do not change because ρ^2 is constant. Thus we consider the conditions for applying Eq. (3) to the BR picture. In the Gutzwiller theory, \bar{v} atoms are doubly occupied with a probability $\eta^{\bar{v}}$, where $0 < \eta < 1$.⁷ In the BR picture¹ at half filling $\rho = 1$ and $\rho_\uparrow = \rho_\downarrow = \frac{1}{2}$, $\eta = \bar{v}/(0.5 - \bar{v})$, and hence $0 < \bar{v} < 1/4$. For the lowest energy state, $\bar{v} = (1/4)(1 - \kappa)$ where $U/U_c = \kappa$, the above limits for \bar{v} imply $0 < \kappa < 1$. When $\rho < 1$ and $\rho_\uparrow = \rho_\downarrow = \frac{1}{2}\rho$, the BR picture can be applied as well, with U averaged over all sites. Since the lowest energy state, $\bar{v} = (1/4)(1 - \kappa\rho^2)$ where $U/U_c = \kappa\rho^2$, is satisfied for $0 < \bar{v} < 1/4$, the condition $0 < \kappa\rho^2 < 1$ is reached. Thus the inverse of the discontinuity q in the BR picture,

$$\frac{1}{q} = \frac{m^*}{m} = (1 - (\frac{U}{U_c})^2)^{-1}, \quad (4)$$

$$= (1 - \kappa^2 \rho^4)^{-1}, \quad (5)$$

where m^* is the effective mass of a quasiparticle, is defined under the combined condition $0 < \kappa\rho^2 < 1$, although the separate conditions are $0 < \rho \leq 1$ and $0 < \kappa \leq 1$. Therefore, m^* increases without bound when $\kappa \rightarrow 1$, $\rho \rightarrow 1$. For $\kappa \neq 0$ and $\rho \rightarrow 0+$, m^* decreases and, finally, the correlation undergoes a (normal or band-type) MIT which differs from the Mott MIT exhibiting a first order transition. For $\rho = 1$, Eq. (5) reduces to the effective mass in the BR picture. At $\kappa\rho^2 = 1$, the MIT of the first order occurs and the state can be regarded as the paramagnetic insulating state because $\bar{v} = 0$. Eq. (5) is illustrated in Fig. 1 (a). In addition, the expectation value of the energy in the (paramagnetic) ground state is given by $\langle H \rangle_N = \bar{e}(1 - \kappa\rho^2)^2$. Here, the band energy $\bar{e} = \bar{e}_\uparrow + \bar{e}_\downarrow = 2\sum_{k < k_F} \epsilon_k < 0$ is the average energy

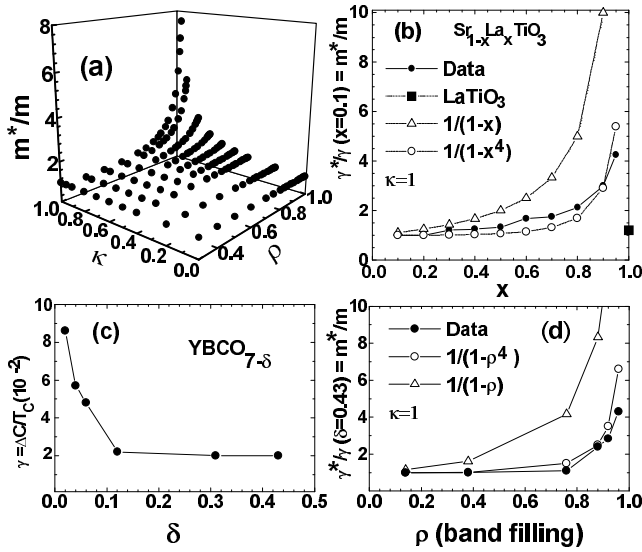


FIG. 1. (a) The effective mass, $\frac{m^*}{m} = \frac{1}{1-\kappa^2\rho^4}$. (b) Experimental data (\bullet) of the heat capacity for $\text{Sr}_{1-x}\text{La}_x\text{TiO}_3$ presented by Tokura⁵ and Kumagai⁶, and a comparison between $\frac{m^*}{m} = \frac{1}{1-x}$ calculated from the $t-J$ model (Δ) and $\frac{m^*}{m} = \frac{1}{1-x^4}$ (\circ). Here, ρ corresponds to x because the number of quasiparticles with x agrees with that of quasiparticles obtained from the Hall coefficient.⁵ Here, $\kappa=1$ and $0 < \kappa\rho^2 < 1$. (c) The heat-capacity coefficient ($\Delta c/T_c$) obtained by magnetic measurements for $\text{YBa}_2\text{Cu}_3\text{O}_{7-\delta}$ superconductors by Daümling.⁸ (d) In the cases $\delta=0$ and $\delta=0.45$, the band is assumed as full with $\rho=1$ and empty with $\rho=0$, respectively. Thus $\rho=1-\delta/0.45$. Here, $\kappa=1$ and $0 < \kappa\rho^2 < 1$.

without correlation and ϵ_k is the kinetic energy in the Hamiltonian in the BR picture¹, with the zero of energy chosen so that $\sum_k \epsilon_k = 0$. This picture may be called an extended BR picture with band filling.

On the other hand, in the $d = \infty$ Hubbard model², in which the width of the DOS $\rho(\omega)$ of the coherent part with a constant peak scale decreases with increasing U , the Mott transition occurs for the *minimum* number of quasiparticles, which number is an integral of $\rho(\omega)$ near $U = U_c$ to energies near $\omega = 0$. This is a marked difference from the BR picture in which the Mott transition occurs at $\rho=1$ (the *maximum* number of quasiparticles). The Mott transition in the $d = \infty$ Hubbard model can be regarded as the band-type MIT in the extended BR picture because of the decrease of the number of quasiparticles in the coherent part. In addition, the $t-J$ model³ and the Hubbard model⁴ on a square lattice predict critical behavior according to $m^*/m = 1/(1-x)$.

Eq. (5) is applied to the heat capacity data of the $\text{Sr}_{1-x}\text{La}_x\text{TiO}_3$, which is well known as a strongly correlated system. The number of quasiparticles determined by the Hall coefficient increases linearly with x up to at least $x=0.95$.^{5,6} The heat capacity in Fig. 3 of reference 5 is replotted, as shown in Fig. 1(b). Eq. (5) follows closely

the heat capacity data in the case when $\kappa=1$. The first-order transition is found between $x=0.95$ and $x=1$. This transition corresponds to the Mott MIT because $\kappa\rho^2 = 1$ in this picture, with $\rho = 1$ at LaTiO_3 and $\kappa = 1$ from the experimental result. Thus LaTiO_3 is a Mott insulator.

Eq. (5) is also applied to the specific heat data for YBCO measured by magnetic measurements by Daümling⁸. Eq. (5) seems to follow the data, as shown in Fig. 1(d). Although it is difficult to confirm whether YBCO at $\rho=1$ is a Mott insulator because the effective mass at $\rho=1$ is divergent, the divergence is regarded as a Mott transition.

We conclude from experimental data that the correlation strength is found to be $\kappa=1$, and that the presently proposed extended BR picture is better able to explain the Mott transition than Hubbard models. Further, instead of the van Hove singularity (vHs), Eq. (5) can be used for 2D-DOS to describe the mechanism of high- T_c superconductivity.

I thank Mr. Nishio for valuable comments, and Prof. Tokura, Prof. Kumagai, and Dr. M. Daümling for permission to use experimental data in Fig. 1(b),(c).

* Physica C **341-348**, 259-260 (2000).

** kimht45@hotmail.com: htkim@etri.re.kr.

¹ W. F. Brinkman and T. M. Rice, Phys. Rev. B **2**, 4302 (1970).

² X. Y. Zhang, M. J. Rozenberg, and G. Kotliar, Phys. Rev. Lett. **70**, 1666 (1993).

³ M. Kawakami and S. K. Yang, Phys. Rev. Lett. **65**, 2309 (1990).

⁴ N. Furukawa and M. Imada, J. Phys. Soc. Jpn. **60**, 3604 (1991).

⁵ Y. Tokura, Y. Taguchi, Y. Okata, Y. Fujishima, T. Arima, K. Kumagai, and Y. Tokura, Phys. Rev. Lett. **70**, 2126 (1993).

⁶ K. Kumagai, T. Suzuki, Y. Taguchi, Y. Okata, Y. Fujishima, and Y. Tokura, Phys. Rev. B **48**, 7636 (1993).

⁷ M. C. Gutzwiller, Phys. Rev. **137**, A1726 (1965).

⁸ Manfred Daümling, physica C **183**, 293 (1991).